Journal of Hazardous Materials 196 (2011) 101–108

Contents lists available at SciVerse ScienceDirect

Journal of Hazardous Materials

journal homepage: www.elsevier.com/locate/jhazmat

Water-soluble organo-building blocks of aminoclay as a soil-flushing agent for heavy metal contaminated soil

Young-Chul Lee[a], Eun Jung Kim[b], Dong Ah Ko[a], Ji-Won Yang[a,b,*]

[a] Department of Chemical and Biomolecular Engineering (BK21 program), KAIST, 335 Gwahak-ro, Yuseong-gu, Daejeon 305-701, Republic of Korea
[b] Advanced Biomass R&D Center, KAIST, 291 Daehakno, Yuseong-gu, Daejeon 305-701, Republic of Korea

ARTICLE INFO

Article history:
Received 12 April 2011
Received in revised form 28 August 2011
Accepted 31 August 2011
Available online 6 September 2011

Keywords:
Heavy metals
Soil flushing
Water-soluble clay
Phyllosilicate
Remediation

ABSTRACT

We demonstrated that water-soluble aminopropyl magnesium functionalized phyllosilicate could be used as a soil-flushing agent for heavy metal contaminated soils. Soil flushing has been an attractive means to remediate heavy metal contamination because it is less disruptive to the soil environment after the treatment was performed. However, development of efficient and non-toxic soil-flushing agents is still required. We have synthesized aminoclays with three different central metal ions such as magnesium, aluminum, and ferric ions and investigated applicability of aminoclays as soil flushing agents. Among them, magnesium (Mg)-centered aminoclay showed the smallest size distribution and superior water solubility, up to 100 mg/mL. Mg aminoclay exhibited cadmium and lead binding capacity of 26.50 and 91.31 mg/g of Mg clay, respectively, at near neutral pH, but it showed negligible binding affinity to metals in acidic conditions. For soil flushing with Mg clay at neutral pH showed cadmium and lead were efficiently extracted from soils by Mg clay, suggesting strong binding ability of Mg clay with cadmium and lead. As the organic matter and clay compositions increased in the soil, the removal efficiency by Mg clay decreased and the operation time increased.

1. Introduction

Soil contamination with toxic heavy metals such as copper, zinc, chromium, cadmium, and lead, has been a big concern in many countries due to their adverse health effects [1]. Thousands of sites contaminated with heavy metals need to be remediated in the United States and other countries, which requires new development of effective soil treatment technologies [2–4]. Currently, various soil treatment technologies, including excavation and landfill, isolation, containment, electrokinetics (EK), biological treatment, and soil flushing (washing) have been applied to remediate heavy metal contaminated sites [3–6]. Among them, soil flushing has shown several advantages such as relatively low cost and less environmentally disruptive consequences compared to the conventional excavation and landfill methods [3,4]. Therefore, it has been widely applied to remove heavy metals from contaminated soils. During soil flushing, acids and other solvents have been applied to enhance the performance, which have caused disruption in the soil environment after treatment [7,8]. Thus, chelating agents such as pyridine-2,6-dicarboxylic acid (PDA), *N*-(2-acetamido) iminodiacetic acid (AIA), and ethylenediaminetetraacetic acid (EDTA), or surfactants [9–14] have been widely employed in place of acids and other solvent to extract heavy metals from soils. However, these chelating agents also resulted in problems because of their recalcitrance and the difficulties separating them from the heavy metal cations, which required additional processes for disposal treatment. Recently, a new class of nanoscale water-soluble chelants of poly(amidoamine) (PAMAM) dendrimer in environmental applications was explored in aqueous solutions [15,16] and soils [1,17]. However, these chelants are expensive and need an additional nanofiltration process to recover them. Therefore, development of alternative chelating agents is still required for an environmentally non-destructive and cost-effective remediation process.

Organic–inorganic hybrid nanomaterials have been getting attractions because of their wide applications. Mann et al. have developed 3-aminopropyl functionalized phyllosilicates (aminoclay) by covalent bonding with a central metal ion and sandwiched organo-functionalities via Si–C bonds [18,19] and reported nanocomposites with biomolecules [20–24]. Unfortunately, they do not have focused on environmental areas. Thus, because aminoclay has unique nano-sized and water-soluble properties with a high density of amino groups, it can lead to applications in environmental studies. In addition, its high chelating capacity with metal ions and less toxicity make the aminoclay as an excellent candidate for a soil flushing agent.

* Corresponding author at: Department of Chemical and Biomolecular Engineering (BK21 program), KAIST, 335 Gwahak-ro, Yuseong-gu, Daejeon 305-701, Republic of Korea. Tel.: +82 42 350 3924; fax: +82 42 350 3910.
E-mail address: jiwonyang@kaist.ac.kr (J.-W. Yang).

0304-3894/$ – see front matter.
doi:10.1016/j.jhazmat.2011.08.077

Table 1
Properties of Jumunjin sand, Soil A, B, and C used in this study.

	Density (g/cm^3)	Bulk density (g/cm^3)	Porosity	pH	Organic content (%)	Soil composition (%)		
						Sand (2–0.02 mm)	Silt (0.02–0.002 mm)	Clay (<0.002 mm)
Jumunjin sand	2.320	1.500	0.582	–	0.11	100	0	0
Soil A	2.340	1.521	0.350	5.85	0.6	93.5	2.5	4.0
Soil B	2.286	1.136	0.497	4.00	3.5	75.0	15.0	10.0
Soil C	2.254	0.789	0.650	6.48	12.1	55.0	28.0	17.0

The objective of this study is to demonstrate that aminoclay can be applied as an alternative soil-flushing agent to remediate heavy metals from soils. We synthesized aminoclays with three different central metal ions and investigated heavy metal binding of aminoclays through batch and column experiments.

2. Experimental

2.1. Materials

All chemical used in this study were reagent grade or higher grade and used without further purification. 3-Aminopropyltriethoxysilane (APTES, 99%), ferric chloride hexahydrate, and aluminum chloride hexahydrate were purchased from Sigma–Aldrich (St. Louis, MO, USA) and magnesium chloride hexahydrate (98.0%) was obtained from Junsei Chemical Co., Ltd. (Tokyo, Japan). Cadmium and lead sources were used as chloride counterions (>99%, A.C.S. reagent). The 1000 mg/L standard solutions of cadmium, lead, and magnesium were obtained from Fluka. Ethanol (>99.9%) was purchased from Merck KGaA (Darmstadt, Germany). Centrifugal filters (Amicon® Ultra, 3 kDa) were bought from Millipore. HCl or NaOH standard solutions (1 N or 0.1 N) were used from DAE JUNG (Shiheung, Korea) to adjust the pH of the samples. Double-distilled deionized water (>18 mΩ, DI water) was used through all of the experiments.

2.2. Preparation of hydrophilic aminoclays

An aminopropyl functionalized magnesium phyllosilicate clay was prepared as previously reported [18–24]. The APTES (1.3 mL, 5.63 mmol) was added in a drop-wise manner to a magnesium chloride (0.84 g, 8.82 mmol) in ethanol (40 mL) at room temperature. The molar ratio of Mg to Si was approximately 0.75. The white slurry was formed after 5 min, which was stirred overnight. The precipitate was isolated by centrifugation, washed with ethanol (50 mL) to remove excess magnesium chloride, and dried at 40 °C. Aminoclays with backbones of Fe and Al were also synthesized using the same procedure described above. For brevity, Mg, Al, and Fe backboned aminoclays will be referred to as Mg clay, Al clay, and Fe clay respectively.

2.3. Cadmium and lead binding of Mg clay in batch system

Batch experiments were conducted to determine the maximum binding capacity of the heavy metal cations in Mg clay solution as a function of pH. The Mg clay solution (0.5 g/L) was reacted with 50 mg/L of cadmium or lead solution at various pH values for 1 day where adsorption equilibrium time was confirmed <1 h. Samples were agitated with magnetic stirrer during the reaction. After reactions, all samples were filtered by an Amicon® centrifugal filter (3 kDa) and then analyzed by atomic absorption spectrometry (AAS, Perkin–Elmer). The removal capacity (q) was calculated by

$$\frac{(C_o - C_{filtered}) \times V}{W} = q\,(mg/g)$$

where C_0 and $C_{filtered}$ were the initial and filtered concentrations after centrifugation (mg/L), V (L) was the sample volume, and W was the mass (g) of the Mg clay. The experiments were conducted in triplicate to get a reliable result.

2.4. Mg clay flushing for cadmium or lead contaminated soils

Column flushing experiments were performed with a 30 mm × 160 mm column (Kontes, USA) containing 110 g of Jumunjin sand (20–30 mesh), and Soil A, B, and C. Jumunjin sand was obtained from seashore of east coast of Korea (Jumunjin, Korea) and Soil A, B, and C were collected on a hill site inside of the university (Daejeon, Korea) and their physical properties were artificially controlled to have different sand, silt, and clay contents. The clay and silt contents increased in the order of Soil A < B< C (Table 2). The elemental compositions observed by X-ray fluorescence (XRF) and physical properties of the soils are summarized in Tables 1 and 2, respectively. X-ray diffraction analysis showed that quartz, illite, and albite are the major mineral composition of Soil A, B, and C. Approximately the same loading of each soil was packed in the column by small incremental actions to obtain homogeneous condition with uniform bulk density [25]. And soil column experiment was The schematic diagram of the column experiment in detail was depicted in Fig. 1. The pore volume of the sand in the column was 30 mL. Initially, 20 pore volumes of DI water were pushed through the column in an upward direction at a flow rate of 2 mL/min. Next, the column was contaminated by circulating an initial concentration of approximately 300 mg/L of divalent cadmium and lead, individually, at a flow rate of 1 mL/min to achieve an equilibrium state for 6 h (at pH 7). Then, more than 30 pore volumes of DI water was introduced in an upward direction in order to remove slightly bounded heavy metals from the soil surfaces. As a result, complete saturation with water for the column was achieved. The preloaded Cd^{2+} and Pb^{2+} uptakes for the Jumunjin sand soil were 120 ± 10 and 180 ± 20 mg/kg, respectively. In cases of Soils A, B, and C (order of clay contents: A < B < C), the preloaded concentrations of Pb^{2+} were 1016, 1216, and 1446 mg/kg, respectively, reflecting sorption of heavy metals on soils were highly affected by the characteristics of the soils. This will be further discussed in Section 3.5. For the flushing of

Table 2
Elemental compositions (%) of Jumunjin sand, Soil A, B, and C observed by X-ray fluorescence (XRF) spectrometer in this study.

	Si	Al	K	Fe	Ca	Ti	Cu	S	Mn	Na
Jumunjin	68.4	8.9	12.7	0.992	0.36	0.12	0.065	0.23	–	6.6
Soil A	67.3	13.9	8.95	5.43	2.34	0.936	0.11	0.51	0.11	–
Soil B	42.7	23	9.15	15	3.86	1.39	0.079	0.36	0.34	–
Soil C	46.4	19.2	7.47	18.2	1.2	1.74	0.11	0.66	0.53	–

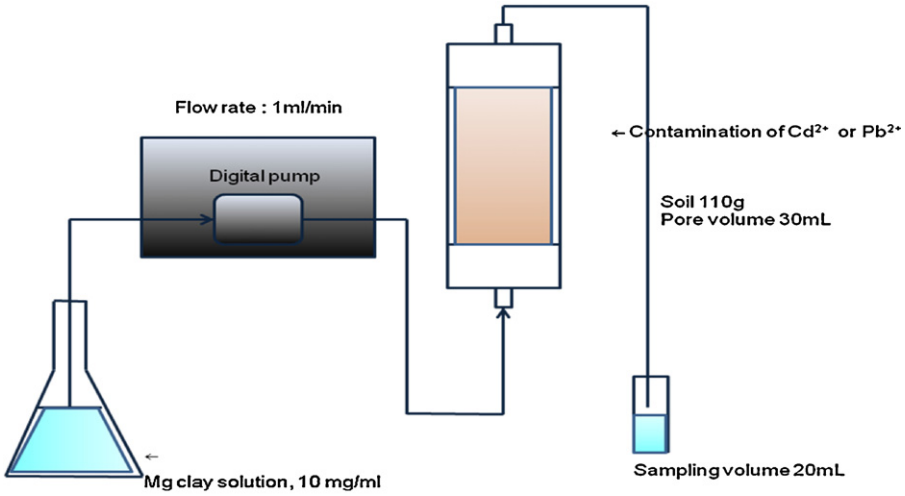

Fig. 1. Schematic presentation of the column experiment for soil flushing.

contaminants from the column, water-soluble Mg clay solutions of 10 mg/mL were pumped in an upward direction through the column at a flow rate of 1 mL/min. After the flushing procedure, residual amounts of Mg clay on the soil were analyzed. During column experiments, flow rate was controlled by a peristaltic pump (Masterflex® L/S®, Cole-Parmer Instrument, USA) [26–28].

2.5. Characterizations

Surface morphology of samples of aminoclays in aqueous media was observed by a transmission electron microscopy (TEM, JEM-2100F, JEOL LTD, Tokyo, Japan). In order to observe TEM samples, tiny amount of aminoclay powder was dispersed in DI water for 5 min sonication, and then subsequently was dropped onto a carbon-coated copper grid. For crystallographic structure of aminoclays, Powder X-ray diffraction (PXRD) data were obtained on a Rigaku D/max lllC (3 kW) with a wide angle goniometer equipped with a CuKα radiation generator at 40 kV and 45 mA, and the scan range was from 3 to 65° at a rate of 1.2° × 2θ/min. Each aminoclay that prepared with mechanical mortar was filled in the holder homogeneously. Zeta potentials of the aminoclay solutions were measured by the Malyern Zetasizer Nano-ZS particle analyzer according to pH. The particle size distributions of aminoclays in aqueous solutions were examined by dynamic light scattering (DLS) method (HELOS/RODOS & SUCELL, Germany). The point of zero charge (PZC) of Soil A, B, and C was measured by titration method [29]. The titration was performed with addition of HCl and KOH (0.1 M), which was corrected by subtraction from the pH of the blank to be required the amounts of acid. To confirm the covalent bonding of central metals and APTES and its organofunctionalities, Fourier transform infrared (FT-IR) spectra of KBr pellets (FT-IR 4100, Jasco, Japan) were collected from 4000 cm^{-1} to 540 cm^{-1}. Each spectrum was recorded as the average of 32 scans with a resolution of 4 cm^{-1}. The pellet disks consisted of 10% aminoclay powder and 90% KBr by weight. The compositions of the Mg clay, Jumunjin sand, and Soil A, B, and C were examined by X-ray fluorescence (XRF, MiniPal2, PANalytical) and an elemental analysis analyzer (EA1108 andNA2000, CEinstrument, USA) was used for aminoclays. Along with that, total amine (TN) and protonated amine (ammonium) in aqueous solution were measured by automatic water analyzer (AACS V, Center for Research Facility in Chungnam National University, Daejeon, Korea). The pH was determined using an Orion pH meter (Thermo Orion, model 710, USA).

3. Results and discussion

3.1. Characterizations of aminoclays

Powder X-ray diffraction (PXRD) patterns for the synthesized aminoclays are shown in Fig. 2. The XRD patterns of Mg, Fe, and Al clays showed typical layered organoclay structure, *i.e.*, d_{001} = 1.5 – 1.8 nm, which corresponded to the previous results [30]. In addition, 2θ = 59° was a distinct peak in the Mg clay, which indicated a 2:1 trioctahedral phyllosilicate ratio. Al and Fe clays had a similar 2:1 dioctahedral phyllosilicates ratio or 1:1 phyllosilicate [30,31]. The main functional groups of aminoclays were characterized as $–CH_2$, $–NH_2$, Si–O, Si–O–Si, and metal-O by Fourier transform infrared (FT-IR) spectroscopy (Fig. 3). All aminoclays formed covalent bonds with the metal ions and organo-functionalities, further $–NH_2$, and protonated $–NH_3^+$ peaks appeared [18,20,24]. X-ray fluorescence (XRF) study showed that Mg-, Al-, and Fe-clay were composed of metal (Mg: 13.0%, Al: 11.8%, and Fe: 43.5%), Si (24.0%, 31.6%, and 26%), and Cl (63.0%, 56.6%, and 30.9%), respectively, which were calculated by summation of three compositions of each metal, Si, and Cl is 100 wt%. Elemental analysis (EA) determined the compositions of C, H, O, and N of Mg clay were 18.3%, 5.6%, 9.4% and 6.7%, respectively. Furthermore, N (%)

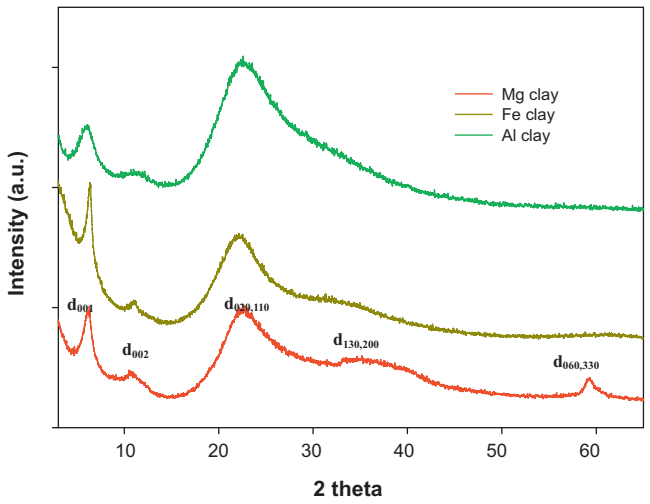

Fig. 2. Powder X-ray diffraction (PXRD) patterns of aminoclays.

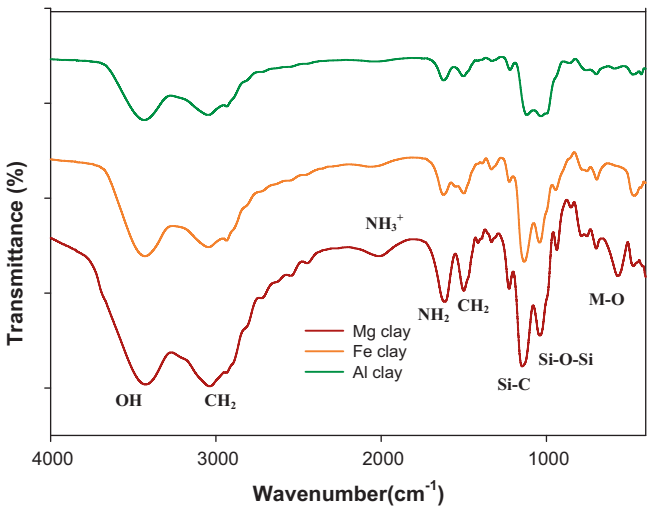

Fig. 3. Fourier transform infrared (FT-IR) spectra of aminoclays. M is denoted as metal.

compositions of Al and Fe clay were 7.91% and 8.20%. From the composition results above, the density of the amino groups of bulk powder of aminoclays was calculated as 4.78 mmol, 5.65 mmol, and 5.86 mmol of nitrogen/g of Mg clay, Al clay, and Fe clay respectively. In order to examine detailed amine function of aminoclays in aqueous solution, total amine (TN) and protonated amine (ammonium form, $-NH_3^+$) concentrations in aqueous solution (pH 5–6) were measured. The TN concentrations of Mg-, Al-, and Fe-clay were 97.21×10^{-3}, 85.95×10^{-3}, and 86.50×10^{-3} mg/L, respectively. The protonated amine concentrations of each clays were 3.78×10^{-3}, 7.04×10^{-3}, and 10.48×10^{-3} mg/L. Interestingly, among the aminoclays, Mg clay in aqueous solution showed highest amine concentration, whereas it showed lowest concentration of protonated amine ($-NH_3^+$), which was not proportional to N density (mmol) by EA. Zeta potential of aminoclays showed positive values of +20–25 mV, while talc, which is a parent mineral of Mg clay, had negative potential (Fig. 4a). Even with increased Mg clay loading, no significant increase of zeta potential occurred (data not shown). As illustrated in Fig. 4b, the positive value of the zeta potential decreased to approximately half of the maximum value, *i.e.*, +5–10 mV, near neutral pH, corresponding to reported dendrimer (~+5 mV) [15,16]. The pH of Al clay in aqueous solution exhibited neutral pH while other clays in aqueous solution showed an approximate pH of 9.8 at 1.5 g/L of clay loading.

Table 3
Particle size distributions of aminoclays.

	Mg clay	Al clay	Fe clay
X_{10}	24.73 nm	269.69 nm	72.90 nm
X_{50}	31.87 nm	320.56 nm	92.42 nm
X_{90}	41.08 nm	370.93 nm	117.03 nm
X_{99}	50.49 nm	394.09 nm	141.67 nm
SMD	31.27 nm	315.84 nm	90.93 nm
VMD	32.49 nm	320.39 nm	94.02 nm
Sv	191.89 m^2/cm^3	19.00 m^2/cm^3	65.99 m^2/cm^3

X_{10}%, X_{50}%, and X_{90}% are the cumulative probability sizes at 10%, 50%, and 90%, abbreviations of surface mean diameter and volume mean diameter are SMD and VMD, Sv is the ratio of SMD and VMD.

3.2. Screening of soil flushing agents

The size distributions of aminoclays observed by dynamic light scattering (DLS) are presented in Table 3. For the Mg clay, the 99% cumulative probability size (X_{99}) was 50.49 nm and the ratio of the surface area mean diameter (SMD) and volume mean diameter (VMD), Sv, was 191.89 m^2/m^3. The higher the value of Sv means the more spherical shape or the smaller particle size. The average diameters (X_{99}) of Al and Fe clays were 394.09 and 141.67 nm, respectively, while the Sv of them were 19.00 and 65.99 m^2/m^3, respectively. Thus, among the clays, Mg clay had the smallest diameter and more spherical shape, suggesting relatively high probability to exist as discrete particles in aqueous solution. The diameter and the shape of the clays were affected by the metal ions of the clay even though they were synthesized under the identical sol-gel reaction with APTES. The discrete dispersion of Mg clay sheets in aqueous solution was confirmed by TEM images, having particle size of 30–200 nm (Fig. 5a). On the other hand, Al clay (Fig. 5b) and Fe clay (Fig. 5c) sheets showed aggregation by stacking, which may be resulted from sample preparation. The smallest size of Mg clay in aqueous phase suggests that the Mg clay might be the most efficient candidate as a soil-flushing agent among the aminoclays when considering the mass transfer between the pores of the soil media. To indirectly observe the solubility of aminoclays in aqueous solution, UV-vis absorption spectra were measured at pH 6 (Fig. 6). Mg and Al clays were highly soluble in aqueous solution in the visible region (400–800 nm of wavelength), even at 10 mg/mL of Mg clay dosage, while Fe clay was more turbid when compared to Mg and Al clays at the same concentration. Based on the size distribution, solubility, amino density, and the zeta potential of aminoclays, we selected Mg clay as a promising candidate for soil flushing and further studied heavy metal binding capacity and soil flushing efficiency of Mg clay in the following sections.

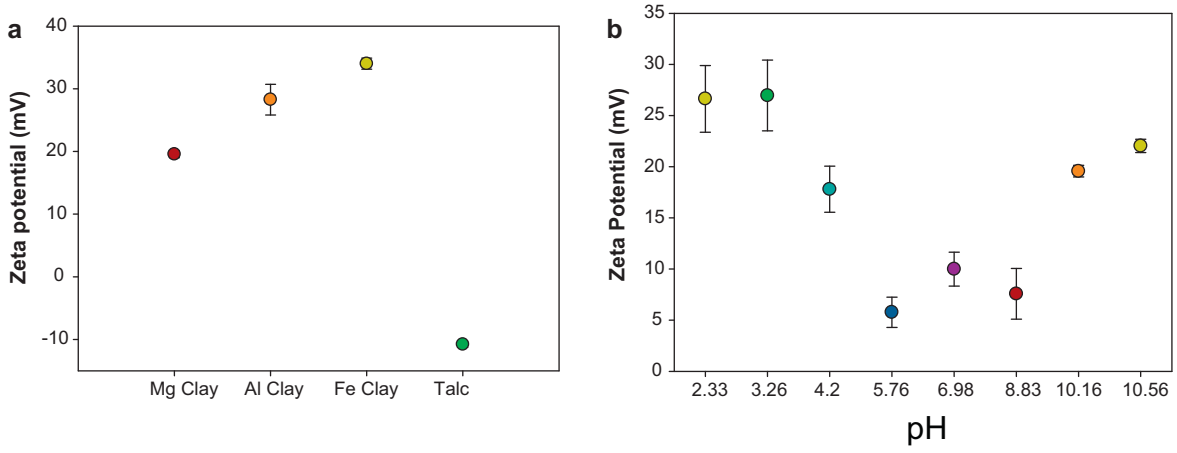

Fig. 4. Zeta potential values of aminoclays (a) at 1.5 g/L of Mg clay as a function of pH (b).

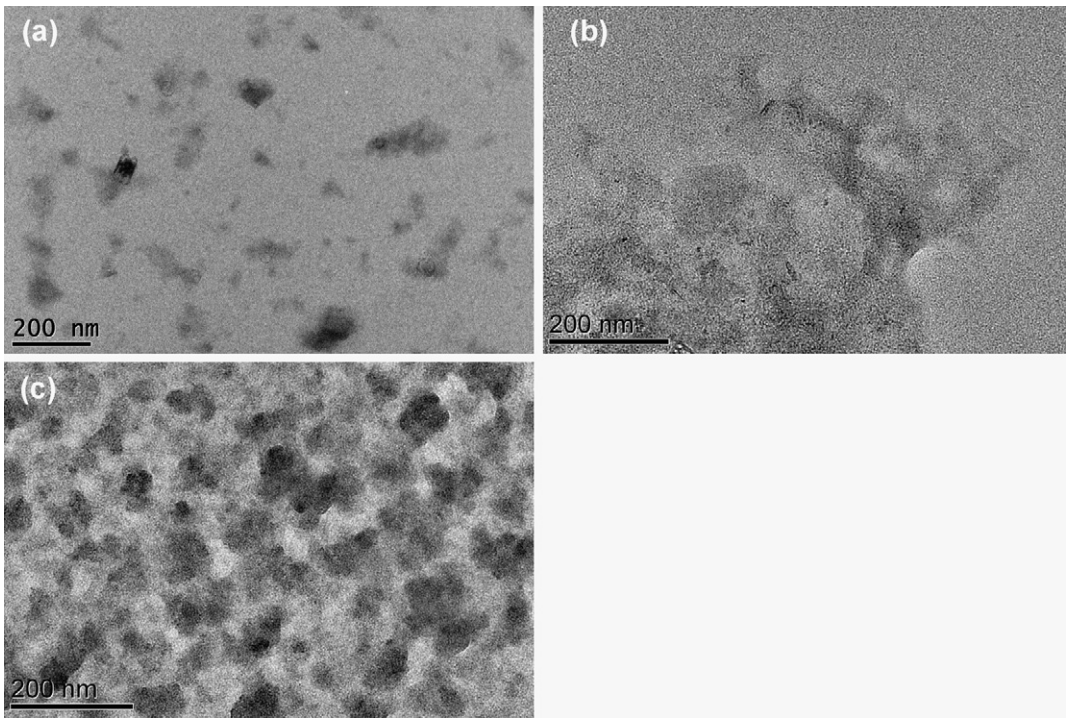

Fig. 5. TEM images of exfoliated dispersions of Mg (a), Al (b), and Fe (c) clay sheets at 1.5 g/L.

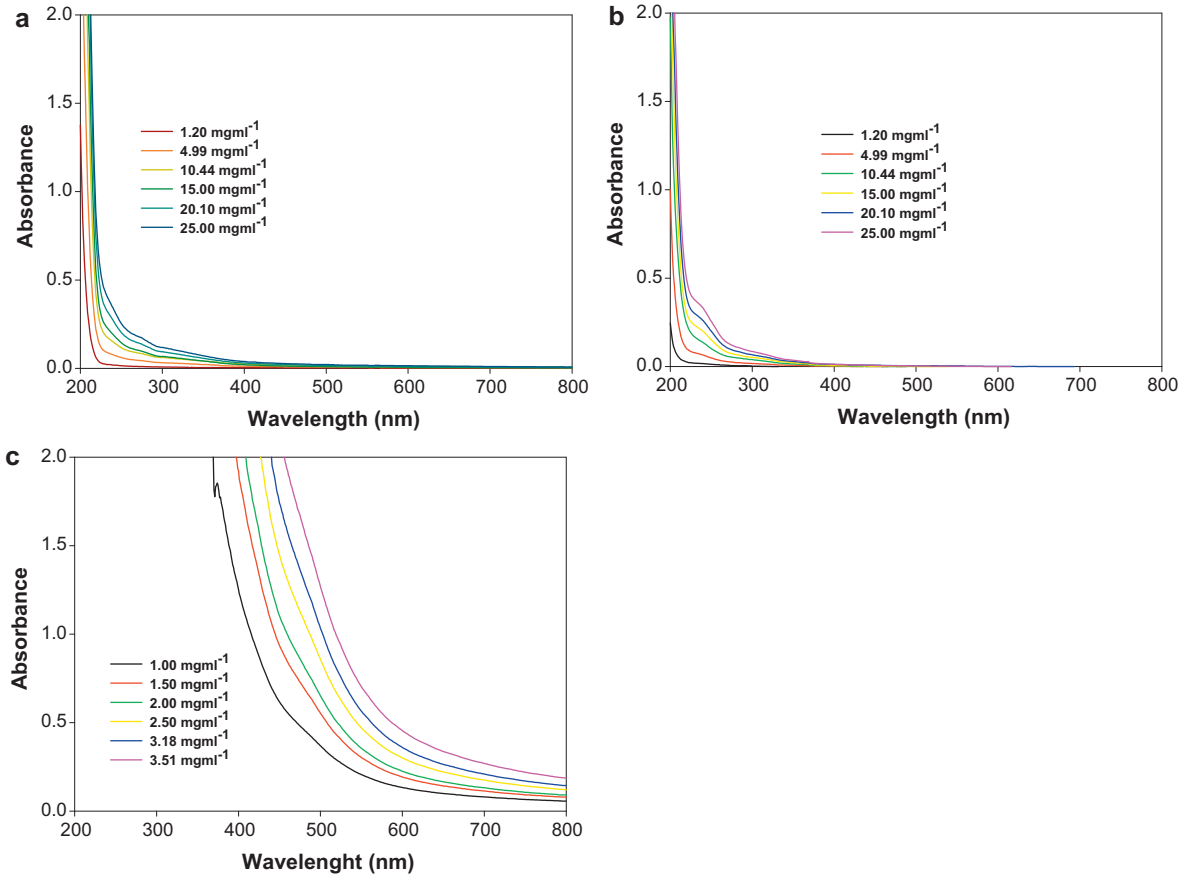

Fig. 6. UV–Vis absorption spectra of Mg clay (a), Al clay (b), and Fe clay (c) as a function of clay loading in aqueous solution.

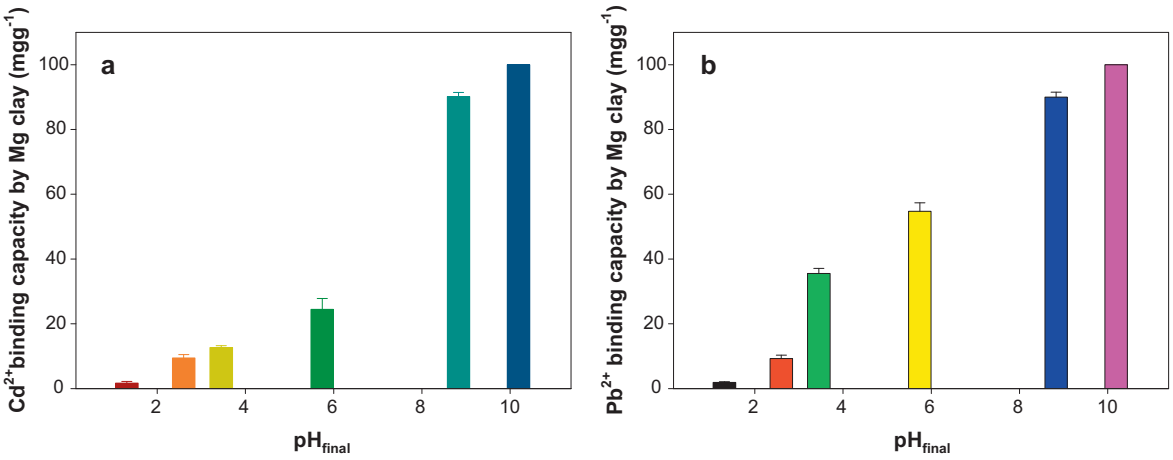

Fig. 7. Binding capacity (q) of cadmium (a) and lead (b) by Mg clay.

3.3. Cadmium and lead binding efficiency (q) with Mg clay in the batch system

Fig. 7 shows a binding capacity of cadmium and lead by Mg clay (0.5 mg/mL) as a function of pH. The cadmium and lead binding capacities of Mg clay were strongly dependent on the solution pH value. The removal of both metals by Mg clay increased as pH increased. However, in case of Cd^{2+}: >pH 8.4 and Pb^{2+}: >pH 6.0 to be plotted by chemical equilibrium modeling of Minteq (version 2.0) (data not shown), the removals of metal ions could be also contributed by alkaline precipitates ($M(OH)_2$, where M = metal ion) as well as binding of Mg clay. Although ionic mobility of Cd^{2+} is higher than that of Pb^{2+} ion at neutral pH by consideration of chemical equilibrium modeling, Mg clay showed higher affinity with lead than cadmium in all pH conditions. Those are in line with amino-functionalized mesoporous material for removal of heavy metals [32–34]. The FT-IR study showed that main functional groups of aminoclays were $-CH_2$, $-NH_2$, Si–O, and Si–O-metal, corresponding to the ideal unit structure of aminoclay [35]. Among the functional groups, heavy metal ions are reported to be well complexed with $-NH_2$ groups. This can be explained that in an acidic condition, Cd^{2+} or Pb^{2+} forms of heavy metals and $-NH_3{}^+$ forms of Mg clay sheets are predominant, resulting in prevention of heavy metal cations adsorbed on Mg clay sheets, but at near neutral pH, free NH_2 of Mg clay sheets can easily chelate on heavy metal ions. Therefore, the uptake of cadmium and lead ions by Mg aminoclay seemed to be mainly contributed by chelating with $-NH_2$ groups of aminoclay. Less protonated NH_2 group in neutral pH is known to better complex with heavy metal ions at near neutral pH [36–39], which explained the higher binding of cadmium and lead ions at near neutral pH. The point of zero charge (PZC) of Mg clay sheets become approximately pH 11.0 [40], indicating that dispersions of Mg clay in DI water shows positive surface potential in wide pH range. The zeta potential (mV) to be dealt in pH range presents +5 to +15 mV. While the measured PZC of Soil A, B, and C used in this study indicates pH 5.4 ± 0.2, 5.0 ± 0.2, and 4.6 ± 0.2, respectively. Thus, heavy metal cations could be loosely bound onto soil surface at near neutral pH due to repulsion with soil surface, this result would be result in higher removal efficiency of heavy metal by Mg clay, which was correlated that free NH_2 groups of Mg clay increased as increase of pH. However, in acidic conditions, the binding was low because of the competition with proton ions. This indicates that Mg clay can be recovered by acid treatment of Mg clay and metal complexes after soil flushing treatment [41].

3.4. Soil-flushing with Mg clay: effect of pH

Fig. 8 shows the effluent concentrations of cadmium and lead extracted from Jumunjin sand soil during soil flushing column experiments with Mg clay as a function of pH. When only DI water was flushed without pH control, the effluent concentration was almost negligible indicating that DI water only did not extract metals from soil. During soil flushing, the effluent Cd^{2+} and Pb^{2+} concentrations increased sharply and at all pH conditions high-

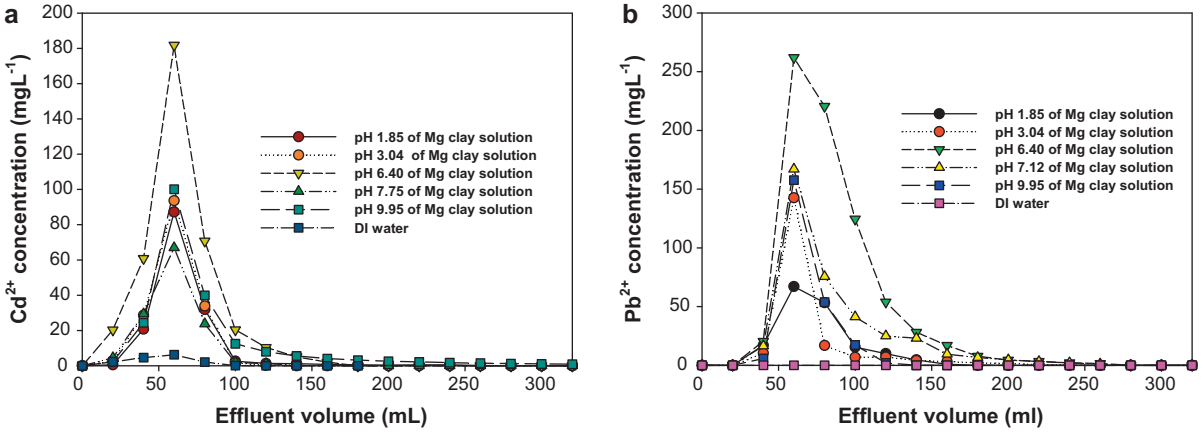

Fig. 8. Mg clay flushing of cadmium (a) and lead (b) contaminated with Jumunjin sand soil.

est concentrations were observed when effluent water volume was 60 mL, which is the two pore volume of the column. This is related to the pore volume of column, approximately 30 mL. After displacing saturated DI water, Mg clay solution collides with heavy metal ions bound onto soil, following that heavy metal ions are directly released out after binding with Mg clay sheets. The cadmium and lead elution from the soil column with Mg clay solution indicates the strong binding ability of Mg clay with cadmium and lead. The removal efficiency of lead by Mg clay was higher than cadmium, which can be explained by higher binding capacity of Mg clay for lead than cadmium as observed in Section 3.3 (Fig. 7). The highest removal efficiency of cadmium and lead was observed at pH 6.4, where the total maximum removal efficiency of cadmium and lead was 61.95% and 83.83%, respectively. Solution pH affected the removal efficiency of cadmium and lead from soil. The pH could affect both availability of metals in soil and affinity to Mg clay. As observed in the previous section, removal of metals by Mg clay increased as pH increased because of increase in free NH_2 of Mg clay. This resulted in increase of the affinity on heavy metal ions with Mg clay where the solubility of Mg clay was negligibly affected. However, metal precipitates could occur at higher pH, which could make hard to elute from the soil. On the other hand, at lower pH the available metal ions increased from the sand soil due to the increased protonation of soil surface, but affinity of metals to Mg clay was also lowered at the same time. In this study, the optimum pH of the soil flushing with Mg clay was observed at pH 6.4 for lead and cadmium ions. In the case of lead, the lowest removal efficiency was observed at the lowest pH, pH 1.85, which suggests that the affinity to Mg clay of lead is more important factor for lead removal efficiency from soil flushing than the available lead in soil. In addition, the shape of the breakthrough curve (BTC) of cadmium elution by Mg clay solution showed symmetry and no tailing without irregularities (Fig. 8a), while lead BTC showed the tailing phenomena. The tailing of the BTC suggests relatively slow mass transfer of lead bounded Mg clay in the soil.

3.5. Soil-flushing with Mg clay: effect of soil properties

In order to investigate the effect of soil properties on soil flushing with Mg clay, soil flushing experiments were conducted with three different types of soils contaminated with lead. We only tested lead-contaminated soil because Mg clay showed better removal efficiency of lead compared to cadmium (Fig. 8). Soil A, B, and C had different physical properties and organic matter contents. The clay and organic matter contents, whose main fraction is humic acid and fulvic mixture, of the soils increased in the order of Soil A, B and C (Table 1). These soils were contaminated with lead and the preloaded lead concentrations were 1016, 1216, and 1446 mg/kg for Soil A, B, and C, respectively. Fig. 9 shows the effluent concentrations of lead extracted from Soil A, B, and C during soil flushing column experiments with Mg clay at pH 6.3, which was the optimum pH of the soil flushing with Mg clay in the previous section. The highest effluent lead concentration was observed for Soil A. About 81% of initially loaded lead on Soil A was removed after soil flushing with Mg clay. The removal efficiencies of Soil B and C were 72.5% and 43.1%, respectively. The preloaded amount of lead on soil increased with the increase of clay and organic matter contents in soil, while the removal efficiency of lead by Mg clay decreased, indicating soil properties affected binding of lead on soil and interactions between lead ions and the removal efficiency of Mg clay. Natural organic matter (humic acid and fulvic acid mixture) and metal oxides such as Mn oxide, Fe oxide, Al oxide, and Ti oxides present in soil have shown to have high affinity for lead [13,42–44]. The XRF study showed that metal oxides as well as sulfates increased in the order of Soil A, B, and C but silicates content did not show a trend (Table 2). The high contents of organic matter, metal oxides, and sulfates in Soil C seemed to make lead more strongly bound to the soils as well as Mg clay was predominantly interacted with organic matters than surrounding anionic metals [45], which results decrease of removal efficiency of Mg clay. Furthermore, slow mass transfer of lead bounded Mg clay occurred in Soil C, which was suggested by obvious tailing phenomena of BTC of Soil C. It took twice longer time (up to 10 h) than flushing of Soil A to reach the time when lead leaching into eluent was stopped. The maximum concentration of lead in the eluent was delayed about one pore volume (30 mL for 20 min). These results suggested that soil properties should be considered for the application to real or weathered heavy metal contaminated soil. Thus, pretreatment of organic matter will be needed prior to application of aminoclay flushing to remediate heavy metals or development of a novel aminoclay by controlling functionalities to interact with heavy metals fast and strongly than with organic matters.

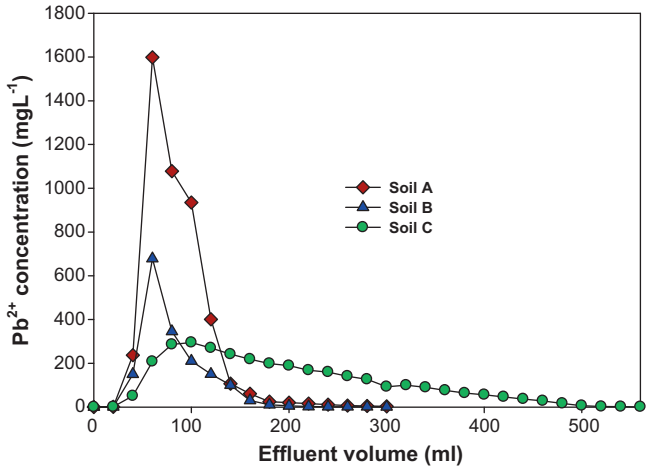

Fig. 9. Mg clay flushing of lead contaminated Soils A, B, and C.

Finally, recovery of Mg clay was calculated after soil flushing. The amounts of Mg clay remained in the Jumunjin sand, Soil A, B, and C after lead flushing were 86 ± 20 mg, 89 ± 30 mg, 92 ± 30 mg, and 95 ± 20 mg, respectively. This indicated that when the organic matter and clay contents in the soil increased, the sorption of Mg clay on soils also slightly increased as sorption of metals on soils. However, the differences were not statistically significant (S.D. = 4.5).

4. Conclusion

In this study, we have synthesized aminoclays with three different central metal ions such as magnesium, aluminum, and ferric ions and investigated applicability of aminoclays as soil flushing agents. Among them, Mg clay showed the smallest size distribution and superior water solubility, which suggests Mg clay as a promising candidate for soil flushing agent due to its efficient mass transfer in soils. In batch experiments, the cadmium and lead binding capacities of Mg clay were best near neutral pH, while at acidic conditions, the binding capacities of them were almost negligible. This indicates that when Mg clay is applied to soil flushing, the pH of the solution should be adjusted to approximately neutral pH to achieve the best performance. In addition, acid treatment process could recover the Mg clay after soil flushing. Due to a high-density of amine groups and water-solubility of Mg clay, it shows a possibility of nanoparticle approaches for the use of soil-flushing agents, instead of molecular (ion) applications such as surfactants, acid, and base agents. Moreover, various aminoclays with a higher amino-density can be applied to enhance removal efficiency. Especially when consideration of soils with high contents of organic matter,

a design of novel aminoclays interacted with heavy metals more strongly is in progress.

Acknowledgements

This subject is supported by Korea Ministry of Environment as "Converging technology project (2010)" and supported by the Advanced Biomass R&D Center (ABC) of Korea Grant funded by the Ministry of Education, Science and Technology (ABC-2010-0029728).

References

[1] Y. Xu, D. Zhao, Removal of lead from contaminated soils using poly(amidoamine) dendrimers, Ind. Eng. Chem. Res. 45 (2006) 1758–1765.
[2] J. Aguado, J.M. Arsuaga, A. Arencibia, M. Lindo, V. Gascón, Aqueous heavy metals removal by adsorption on amine-functionalized mesorporou silica, J. Hazard. Mater. 163 (2009) 213–221.
[3] Y. Xu, D. Zhao, Removal of copper from contaminated soil by use of poly(amidoamine) dendrimers, Environ. Sci. Technol. 39 (2005) 2369–2375.
[4] G. Dermont, M. Bergeron, G. Mercier, M. Richer-Laflèche, Soil washing for metal removal: a review of physical/chemical technologies and field applications, J. Hazard. Mater. 152 (2008) 1–31.
[5] K. Maturi, K.R. Reddy, Simultaneous removal of organic compounds and heavy metals from soils by electrokinetic remediation with a modified cyclodextrin, Chemosphere 63 (2006) 1022–1031.
[6] C.N. Mulligan, R.N. Yong, B.F. Gibbs, Remediation technologies for metal-contaminated soils and groundwater: an evaluation, Eng. Geol. 60 (2001) 193–207.
[7] T. Makino, K. Sugahara, Y. Sakurai, H. Takano, T. Kamiya, K. Sasaki, T. Itou, N. Sekiya, Remediation of cadmium contamination in paddy soils by washing with chemicals: selection of washing chemicals, Environ. Pollut. 144 (2006) 2–10.
[8] D.A. Clifford, M. Yang, T. Nedwed, Feasibility of extracting toxic metals from soil using anhydrous ammonia, Waste Manag. 13 (1993) 207–219.
[9] I.M.C. Lo, X.Y. Yang, EDTA extraction of heavy metals from different soil fractions and synthetic soils, Water Air Soil Pollut. 109 (1999) 219–236.
[10] M.A.M. Kedziorek, A. Dupuy, A.C.M. Bourg, F. Compère, Leaching of Cd and Pb from a polluted soil during the percolation of EDTA: laboratory column experiments modeled with a non-equilibrium solubilization step, Environ. Sci. Technol. 32 (1998) 1609–1614.
[11] L.D. Palma, P. Ferrantelli, F. Medici, Heavy metals extraction from contaminated soil: recovery of the flushing solution, J. Hazard. Mater. 77 (2005) 205–211.
[12] L.D. Palma, P. Ferrantelli, C. Merli, F. Biancifiori, Recovery of EDTA and metal precipitation from soil flushing solutions, J. Hazard. Mater. B103 (2003) 153–168.
[13] C.N. Mulligan, R.N. Yong, B.F. Gibbs, Surfactant-enhanced remediation of contaminated soil: a review, Eng. Geol. 60 (2001) 371–380.
[14] R.W. Peters, Chelant extraction of heavy metals from contaminated soils, J. Hazard. Mater. 66 (1999) 151–210.
[15] M.S. Diallo, L. Balogh, A. Shafagati, J.H. Johnson Jr., W.A. Goddard III, D.A. Tomalia, Poly(amidoamine) dendrimers: a new class of high capacity chelating agents for Cu(II) ions, Environ. Sci. Technol. 33 (1999) 820–824.
[16] M.S. Diallo, S. Christie, P. Swaminathan, J.H. Johnson Jr., W.A. Goddard III, Dendrimer enhanced ultrafiltation. 1. Recovery of Cu(II) from aqueous solutions using PAMAM dendrimers with ethylene diamine core and terminal NH_2 groups, Environ. Sci. Technol. 39 (2005) 1366–1377.
[17] L.D. Palma, F. Medici, Recovery of copper from contaminated soil by flushing, Waste Manage. 22 (2002) 883–886.
[18] S.L. Burkett, A. Press, S. Mann, Synthesis, characterization, and reactivity of layered inorganic–organic nanocomposites based on 2:1 trioctahedral phyllosilicates, Chem. Mater. 9 (1997) 1071–1073.
[19] S. Mann, S.L. Burkett, S.A. Davis, C.E. Fowler, N.H. Mendelson, S.D. Sims, D. Walsh, N.T. Whilton, Sol–gel synthesis of organized matter, Chem. Mater. 9 (1997) 2300–2310.
[20] A.J. Patil, E. Muthusamy, S. Mann, Synthesis and self-assembly of organoclay wrapped biomolecules, Angew. Chem. Int. Ed. 43 (2004) 4928–4933.
[21] A.J. Patil, E. Muthusamy, S. Mann, Fabrication of functional protein-organoclay lamellar nanocomposites by biomolecules-induced assembly of exfoliated aminopropyl-functionalized magnesium phyllosilicates, J. Mater. Chem. 15 (2005) 3838–3843.
[22] K.M. Bromley, A.J. Patil, A.M. Seddon, P. Booth, S. Mann, Bio-functional mesolamellar nanocomposites based on inorganic/polymer interaction in purple membrane (Bacteriorhodopsin) films, Adv. Mater. 19 (2007) 2433–2438.
[23] S.C. Holmström, A.J. Patil, M. Butler, S. Mann, Influence of polymer co-intercalation on guest release from aminopropyl-functionalized magnesium phyllosilicate mesolamellar nanocomposites, J. Mater. Chem. 17 (2007) 3894–3900.
[24] Y.-C. Lee, T.-H. Lee, H.-K. Han, W.J. Go, J.-W. Yang, H.-J. Shin, Optical properties of fluorescein-labeled organoclay, Photochem. Photobiol. 86 (2010) 520–527.
[25] I.M.C. Lo, D.C.W. Tsang, T.C.M. Yip, F. Wang, W. Zhang, Significance of metal exchange in EDDS-flushing column experiments, Chemosphere 83 (2011) 7–13.
[26] Y.-C. Lee, T.-S. Kwon, J.-S. Yang, J.-W. Yang, Remediation of groundwater contaminated with DNAPLs by biodegradable oil emulsion, J. Hazard. Mater. 140 (2007) 340–345.
[27] S.R. Kanel, D. Nepal, B. Manning, H. Choi, Transport of surface-modified iron nanoparticle in porous media and application to arsenic (III) remediation, J. Nanopart. Res. 9 (2007) 725–735.
[28] Y.-C. Lee, C.-W. Kim, J.-Y. Lee, H.-J. Shin, J.-W. Yang, Characterization of nanoscale zero valent iron modified by nonionic surfactant for trichloroethylene removal in the presence of humic acid: a research note, Desal. Water Treat. 10 (2009) 33–38.
[29] C. Taubaso, M.D.S. Afonso, R.M.T. Sánchez, Modelling soil surface charge density using mineral composition, Geoderma 121 (2004) 123–133.
[30] A.J. Patil, S. Mann, Self-assembly of bio-inorganic nanohybrids using organoclay building blocks, J. Mater. Chem. 18 (2008) 4605–4615.
[31] B. Lebeau, J. Brendlé, C. Marichal, A.J. Patil, E. Muthusamy, S. Mann, One-step synthesis and solvent-induced exfoliation of hybrid organic–inorganic phyllosilicate-like materials, J. Nanosci. Nanotechnol. 6 (2006) 352–359.
[32] J. Aguado, J.M. Arsuaga, A. Arencibia, M. Lindo, V. Gascón, Aqueous heavy metals removal by adsorption on amine-functionalized mesoporous silica, J. Hazard. Mater. 163 (2009) 213–221.
[33] J. Wang, S. Zheng, Y. Shao, J. Liu, Z. Xu, D. Zhu, Amino-functionalized Fe_3O_4@SiO_2 core-shell magnetic nanomaterial as a novel adsorbent for aqueous heavy metals removal, J. Colloid Interface Sci. 349 (2010) 293–299.
[34] L. Zhang, C. Yu, W. Zhao, Z. Hua, H. Chen, L. Li, J. Shi, Preparation of multi-amine-grafted mesoporous silicas and their application to heavy metal ions adsorption, J. Non-Cryst. Solids 353 (2007) 4055–4061.
[35] H.-K. Han, Y.-C. Lee, M.-Y. Lee, A.J. Patil, H.-J. Shin, Magnesium and calcium organophyllosilicates: synthesis and in vitro cytotoxicity study, ACS Appl. Mater. Interfaces 3 (2011) 2564–2572.
[36] M.G. da Fonseca, C. Airoldi, New layered inorganic–organic nanocomposites containing *n*-propylmercapto copper phyllosilicates, J. Mater. Chem. 10 (2000) 1457–1463.
[37] M.G. da Fonseca, E.C. da Silva Filho, R.S.A. Machado Junior, L.N.H. Arakaki, J.G.P. Espinola, C. Airoldi, Zinc phyllosilicates containing amino pendant groups, J. Solid State Chem. 177 (2004) 2316–2322.
[38] A. Dong, J. Xie, W. Wang, L. Yu, Q. Liu, Y. Yin, A novel method for amino starch preparation and its adsorption for Cu(II) and Cr (VI), J. Hazard. Mater. 181 (2010) 448–454.
[39] A.E. Martell, R.D. Hancock, Metal Complexes in Aqueous Solutions, Plenum press, New York, London, 1996.
[40] P. Chaturbedy, D. Jjagadeesan, M. Eswaramoorthy, pH-sensitive breathing of clay within the polyelectrolyte matrix, ACS Nano 4 (2010) 5921–5929.
[41] H. Yoshitake, T. Yokoi, T. Tatsumi, Adsorption behavior of arsenate at transition metal cations captured by amino-functionalized mesoporous silicas, Chem. Mater. 15 (2003) 1713–1721.
[42] Y. Xu, T. Boonfueng, L. Axea, S. Maeng, T. Tyson, Surface complexation of Pb(II) on amorphous iron oxide and manganese oxide: spectroscopic and time studies, J. Colloid Interface Sci. 299 (2006) 28–40.
[43] R.M. Town, M. Filella, Implications of natural organic matter binding heterogeneity on understanding lead(II) complexation in aquatic systems, Sci. Tot. Environ. 300 (2002) 143–154.
[44] H.B. Bradl, Adsorption of heavy metal ions on soils and soils constituents, J. Colloid Interface Sci. 277 (2004) 1–18.
[45] Y.-C. Lee, W.-K. Park, J.-W. Yang, Removal of anionic metals by amino–organoclay for water treatment, J. Hazard. Mater. 190 (2011) 652–658.